An Ultrasonically Powered System Using an AlN PMUT Receiver for Delivering Instantaneous mW-Range DC Power to Biomedical Implants

Rashidi, Amin; Saccher, Marta; Karuthedath, Cyril Baby; Sebastian, Abhilash Thanniyil; Savoia, Alessandro Stuart; Lavigne, Frederik; Stubbe, Frederic; Dekker, Ronald; Giagka, Vasiliki

DOI
10.1109/IUS51837.2023.10306557

Publication date
2023

Document Version
Final published version

Published in
Proceedings of the 2023 IEEE International Ultrasonics Symposium (IUS)

An Ultrasonically Powered System Using an AlN PMUT Receiver for Delivering Instantaneous mW-Range DC Power to Biomedical Implants

Amin Rashidi*, Marta Saccher*, Cyril Baby Karuthedath **, Abhilash Thanniyil Sebastian**,
Alessandro Stuart Savoia§, Frederik Lavigne¶, Frederic Stubbe ¶, Ronald Dekker *‖, and Vasiliki Giagka *‡
* Department of Microelectronics, Delft University of Technology, Delft, The Netherlands
† imec-Holst Centre, Eindhoven, The Netherlands
** VTT Technical Research Centre of Finland, Espoo, Finland
§ Department of Industrial, Electronic, and Mechanical Engineering, Roma Tre University, Rome, Italy
¶ Cyient, Leuven, Belgium
‖ MEMS & Micro Devices, Philips, Eindhoven, The Netherlands
‡Technologies for Bioelectronics Group, Fraunhofer Institute for Reliability and Microintegration IZM, Berlin, Germany
Email: a.rashidi@ieee.org, Cyril.Karuthedath@vtt.fi, V.Giagka@tudelft.nl

2023 IEEE International Ultrasonics Symposium (IUS) | 979-8-3503-4645-9/23/$31.00 ©2023 IEEE | DOI: 10.1109/IUS51837.2023.10306557

***Abstract*—Aluminum Nitride (AlN) Piezoelectric Micromachined Ultrasonic Transducers (PMUTs) are gaining interest for biomedical implant power due to biocompatibility and low-temperature processing. However, due to the low piezoelectric coefficient of AlN PMUTs, storage capacitors are often used to accumulate ultrasonic power transferred over an extended time. The accumulated energy is then used to power a DC load, which leads to a long start-up time, and insufficient duty cycle for some applications. We present an ultrasonically powered system for biomedical implants capable of delivering mW-range instantaneous power to DC loads, without pre-storing it. The system features a 25 $\mathrm{mm^2}$ AlN PMUT, an inductive matching network, and an application-specific power management integrated circuit(ASIC). For an acoustic intensity of 360 $\mathrm{mW/cm^2}$ at the surface of the PMUT, an open-circuit voltage of 1.11 V and an aperture efficiency of 30.5 % are measured. Furthermore, by connecting a series-matching inductor to the PMUT, the highest-reported power delivered to the load (PDL) of 6.4 mW is measured over an optimal load of 7.6 Ω. Finally, together with the ASIC and at the intensity of 108 $\mathrm{mW/cm^2}$, our system delivers 1.04 mW DC power to a 3.3 kΩ load, which is over two orders of magnitude higher than the previously reported average DC power for AlN PMUTs.**

***Index Terms*—ultrasonic powering, AlN PMUT, matching network, power management, implants**

I. Introduction

Among various wireless power transfer schemes, ultrasonic has shown superior functionality and adaptability for powering mm-sized batteryless systems implanted deep into the body [1]–[3]. However, most of the reported ultrasonically powered implants are equipped with bulk piezoelectric receivers, which are often not biocompatible and require labor-intensive manual integration.Therefore, micromachined ultrasonic transducers (MUTs) have gained interest in powering biomedical implants, recently. MUTs include capacitive (CMUTs), and piezoelectric (PMUTs) versions based on their transduction mechanism. Aluminum Nitride (AlN) is often preferred as the active material of PMUTs utilized in biomedical implants due to its biocompatibility, and low-temperature process [4]–[7].

This work was funded by the ECSEL Joint Undertaking project Moore4Medical, grant number H2020-ECSEL-2019IA-876190.

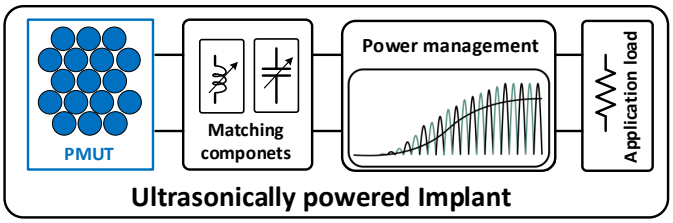

Fig. 1. An ultrasonically powered implant featuring a PMUT receiver

Fig. 1 shows a simplified block diagram of an ultrasonically powered implant with a PMUT receiver, where the application load is modeled by electrical resistance. Since most of the applications require a robust DC supply rail, a power management unit (PMU) is required to rectify the AC power-carrier signal and generate DC supply levels according to the application's needs. While off-the-shelf (OTS) diodes and integrated circuits (ICs) are often used in the literature for prototyping the PMU [5], [6], application-specific integrated circuits (ASICs) can pave the way for monolithic integration of PMUTs on top of ASIC as demonstrated in [4]. Due to the low efficiency of the PMUT-based implants, PMUs in [4] and [6] are equipped with large storage capacitors to accumulate ultrasonic power transferred over an extended time, and then use it to power a DC load. However, this leads to a long start-up time, and a short duty cycle for some applications. To increase the receiving efficiency of PMUTs, matching networks are often used as an interface between the PMUTs and the electrical load seen at their terminals [5], [6]. For this purpose, an inductor-based matching network is commonly used to compensate for the large static capacitance inherent to the majority of micromachined transducers [5], [6]. As an attempt to achieve a smaller footprint, a higher quality factor, and voltage boosting at PMUT terminals, [5] has proposed to use parallel resonators instead of common inductors in matching

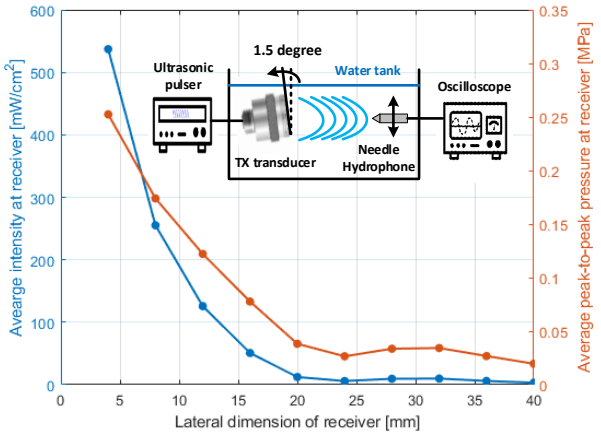

Fig. 2. Degradation of average intensity and peak-to-peak pressure due to 1.5-degree angular misalignment for different RX dimensions.

networks. Even though a smaller footprint is advantageous, the higher quality factors come at the cost of smaller bandwidth, and the so-called voltage boosting effect can be also achieved by a parallel inductor.

In this work, we present an ultrasonically powered system that is capable of delivering a mW-range instantaneous power to a DC load by employing a 25 mm^2 AlN-PMUT, an inductive matching network, and an ASIC for power management.

II. Design Methodology

A. PMUT Design

AlN PMUTs show a rather low receiving efficiency [4]–[6]. Therefore, PMUTs with a larger aperture are required for receiving sufficient energy for more power-demanding applications. However, a larger aperture makes them more sensitive to nonuniform phase distributions and efficiency degradation for small misalignments. Fig. 2 illustrates the degradation of average intensity and peak-to-peak pressure due to a 1.5° angular misalignment of the transmitter for different RX dimensions. The transmitter is a circular single-element PZT piston transducer with a diameter of 39 mm. A needle hydrophone mounted on a motorized stage was used to scan a planar plane with the same area as potential RX transduces. As can be seen in this figure, the small tilt of the TX causes a significant drop in average acoustic intensity from 540 mW/cm^2 to less than 10 mW/cm^2 when increasing the lateral dimensions of the receiver from 4 to 20 mm. The sensitivity of big transducers to angular misalignment is further discussed by the authors in [8]. Therefore, as a trade-off between maximum power delivered to the load (PDL) and lower sensitivity to angular misalignment, an active area of $5\ mm \times 5\ mm$ is chosen for the PMUT.

It has been shown that doping AlN with Scandium (ScAlN) improves the transmitting performance of PMUTs [5]. However, Scandium doping cause higher stress, lower uniformity, and higher cost compared to typical AlN PMUT while it does not necessarily improve receiving efficiency. Therefore, typical AlN PMUTs are designed and fabricated in this work.

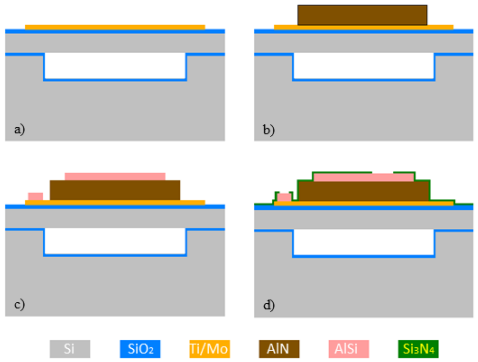

Fig. 3. AlN PMUT fabrication process flow: a) cavity SOI wafer with a thin layer of thermal oxide, with bottom electrode sputter deposited and patterned, b) piezo layer (AlN) deposition, patterning and wet etch, c) AlSi top electrode deposition and patterning, d) thin silicon nitride passivation layer deposition and patterning to open wire bonding contact pads.

B. PMUT Fabrication Process

Figure 3 shows a cross-sectional view of a single PMUT cell and the fabrication process flow. PMUTs are fabricated using Cavity-Silicon on Insulator (C-SOI) wafers. The membrane is composed of a Silicon (Si) structural layer, an AlN piezoelectric material, an Aluminium (Al) top electrode, and a Molybdenum (Mo) bottom electrode. The cavity beneath the silicon structural layer is in vacuum conditions, and the layer thickness is optimized to achieve maximum receive performance. The PMUT fabrication process begins with the growth of a thin thermal oxide layer for electrical isolation, followed by sputter deposition of the Titanium/Molybdenum (Ti/Mo), which is then patterned and etched to define the PMUT bottom electrode (Fig. 3(a)). An AlN piezoelectric layer (1 μm) is then sputter deposited and patterned using an oxide mask and wet etching. (Fig. 3(b)). The bottom electrode and AlN piezoelectric active layers are deposited with an Evatec Clusterline 200 II (CLN 200) sputtering system, and the sputter deposition process parameters are optimized to minimize the residual stress within ±100 MPa. An Aluminum-Silicon (AlSi(1%)) layer is deposited, patterned, and etched to define the PMUT top electrode (Fig. 3(c)). A relatively thick AlSi layer is used as the top electrode metal to reduce the resistance losses. Finally, the PMUT is covered using a thin silicon nitride passivation layer and patterned to open pad regions for wire bonding (Fig. 3(d)).

C. Power Carrier Frequency and Matching Network

To determine the power carrier frequency, we carried out a pulse-echo experiment which is based on measuring the PMUT's open-circuit sensitivity over different frequencies. First, the PMUT's total RX-TX sensitivity is measured using the setup shown in Fig. 4. This is done by driving a pulse to the PMUT array at a 7.5 cm distance from a reflector and measuring the echo with the same array. Then, the TX sensitivity is measured using a hydrophone at the place of the reflector. Finally, the total RX-TX sensitivity is divided by the TX sensitivity to drive the RX sensitivity (normalized to its peak value in Fig. 4). This measurement demonstrates the

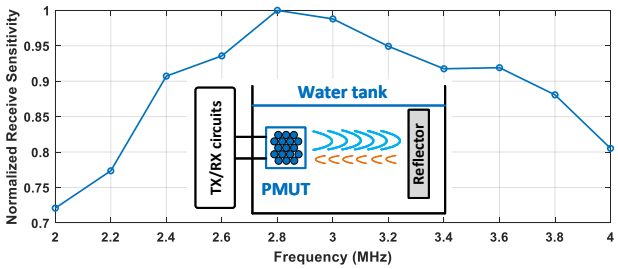

Fig. 4. PMUT's normalized RX sensitivity from the pulse-echo experiment.

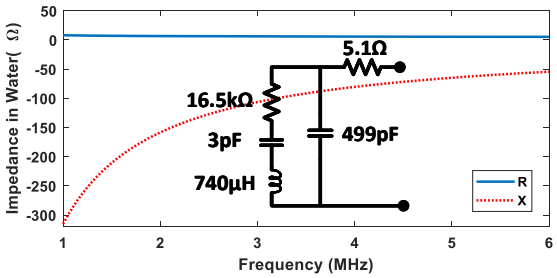

Fig. 5. PMUT's impedance and BVD model in water.

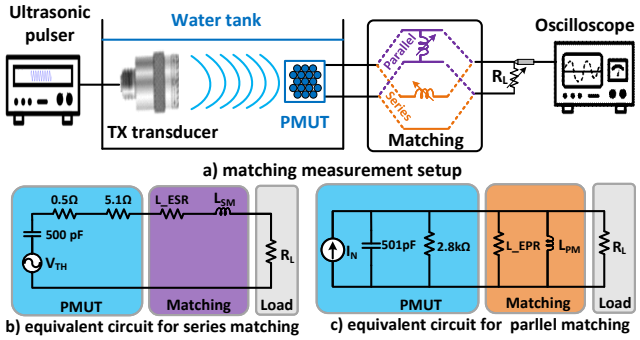

Fig. 6. a) test setup for matching circuits, b) equivalent circuit series matching, and c) equivalent circuit parallel matching.

highest sensitivity (over 90%) in the range of 2.4-3.6 MHz. Thus, 2.5MHz is selected as the carrier frequency due to reduced tissue attenuation at lower frequencies.

In order to design the matching network, the initial step involves measuring the impedance of the submerged PMUT across a frequency spectrum of 1-6 MHz, utilizing a network analyzer. Fig. 5 depicts the measured impedance in conjunction with its fitted Butterworth-Van Dyke (BVD) equivalent model. The 5.1 Ω series resistance (PMUT_ESR) in the model represents the electrical interconnects between the PMUT array and the PADs. Fig. 6(a) shows the matching measurement setup for searching the optimal load in case of series or parallel matching. Here, series matching and parllel matching correspond to scenarios in which the PMUT receiver, the matching inductor, and the resistive load are connected either in parallel or in series, respectively. For further analysis of the two scenarios, the PMUT's impedance is simplified with its Thevenan (Fig. 6(b)) and Norton (Fig. 6(c)) equivalents at the frequency of 2.5 MHz. Furthermore, The limited quality factor (Q) of the matching inductor is modeled with its equivalent

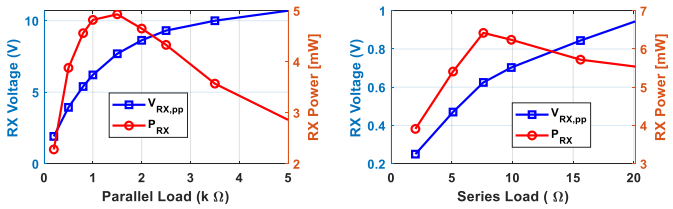

Fig. 7. RX Power and voltage for (a) parallel load, (b) series load.

series or parallel resistance (L_ESR or L_EPR, respectively). Using inductors with Q $\simeq$ 20, the L_ESR $\simeq$ 5 $k\Omega$ and L_EPR $\simeq$ 2.9 $k\Omega$ are calculated for the designed matching inductors. It can be observed from lumped element model in Fig. 6 that in both parallel and series matching scenarios, the parasitic resistances of the PMUT's interconnects and the matching inductors dominate the total source resistance. Therefore, even for a perfect matching half of the power will be dissipated on the parasitic source resistance.

D. Power Management ASIC

Custom-designed power management ICs can pave the way for more efficient and miniaturized implants. Therefore, an ASIC is designed and fabricated in a 180-nm bipolar CMOS DMOS (BCD) technology for generating DC supply voltages using the available electrical power at the implant. The ASIC includes a semi-active rectifier and two programmable voltage regulators at 1.8 V and 3 V levels for generating the DC supply rails required for a variety of applications. The ASIC supports up to 5 V voltage levels and is equipped with overvoltage protection circuits. To limit the ripples at the output of the rectifier, a nF-range storage capacitor is recommended.

III. Results

For an acoustic intensity of (I_{US} = 360 mW/cm^2) at the PMUT's surface with the active area of A = 25 mm^2, an open-circuit peak-to-peak voltage of $V_{RX,pp}$=1.11 V is measured. accordingly, RX ultrasonic power (P_{US}) and available electric power ($P_{av.elec}$) can be formulated as below [1]:

$$P_{US} = I_{US} \times A = 90\ mW \tag{1}$$

$$P_{av.elec} = \frac{{V_{RX,pp}}^2}{8 \times R_{PMUT}} = 27.5mW \tag{2}$$

Thus, the aperture efficiency (η_{apr}) is calculated as:

$$\eta_{apr} = \frac{P_{av.elec}}{P_{US}} = \frac{{V_{RX,pp}}^2}{8 \times R_{PMUT} \times I_{US} \times A} = 30.5\% \tag{3}$$

However, the total receiving efficiency (η_{RX}) is lower due to the matching efficiency (maximum 50 %), and diffraction factor [5]. For measuring η_{RX}, the test setup in Fig. 6 is used at I_{US} = 360 mW/cm^2. Fig. 7 illustrates the RX power and voltage across the load for parallel and series matching. Series matching achieved 6.4 mW power and 7.11 % efficiency with a 7.6 Ω load. Parallel matching reached 4.96 mW power and 5.51 % efficiency over a 1.5-$k\Omega$ resistor. Both cases use 6.2 μH inductance (4.7 μH in series with 1.5 μH

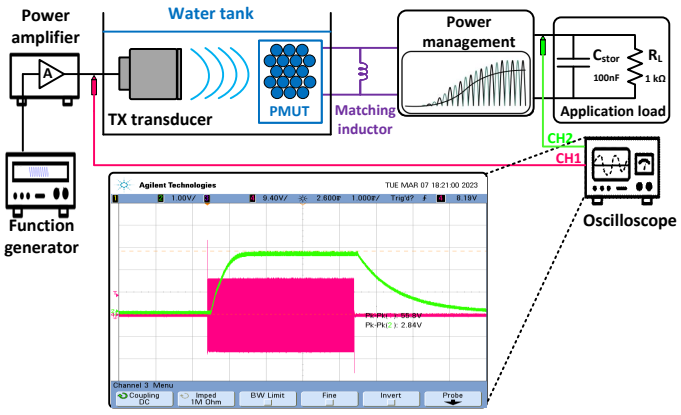

Fig. 8. Schematic of the measurement setup and transient result for the system including ASIC.

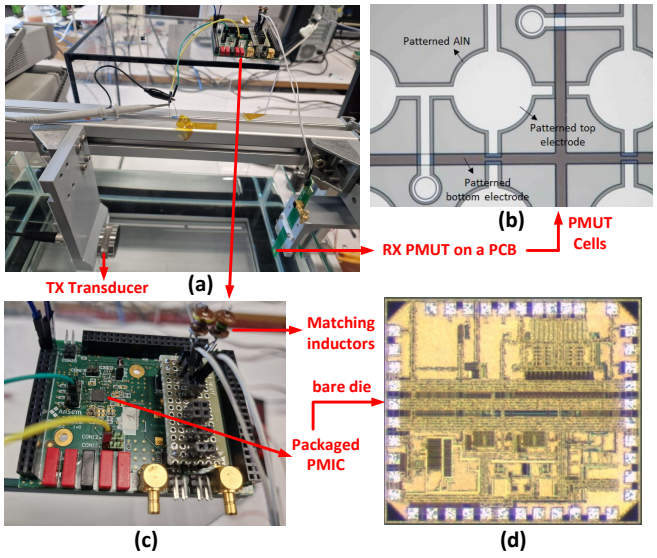

Fig. 9. photos of a) ultrasonic setup, b) the fabricated PMUT cells, c)power management PCB, and d) bare PMIC die

inductors) for the matching component. Fig. 8, and 9 illustrate the schematic and photos of our complete system. As shown in the oscilloscope photo in Fig. 8, our system is capable of continuously powering DC loads upon the availability of ultrasonic energy. At $I_{US} = 108\ mW/cm^2$, DC voltages of 3.9 V, 2.6 V, and 1.85 V were measured for open-circuit, 1 $k\Omega$, and 3.3 $k\Omega$ loads, respectively. Therefore, a maximum of 1.04 mW DC power can be continuously delivered to the 3.3 $k\Omega$ load upon the availability of the ultrasonic link. An optical microscope image of fabricated PMUT cells and fabricated ASIC are shown in Figure 9(b) and (d), respectively. The ASIC occupies a total silicon area of 1640 $\mu m \times 1440\ \mu m$. The fabricated die is packaged in a 5 $mm \times 5\ mm$ QFN package for prototyping purposes (9(c)).

IV. Conclusions

This paper presents an ultrasonically powered system featuring a 25 mm^2 PMUT receiver and a custom-designed power management IC. The design parameters and methodology are discussed in detail. A summary of the specifications and a comparison with the state-of-the-art works are presented in Table I. According to the measurement results, the highest-reported AC power delivered to the load PDL_{AC} among AlN-PMUTs is achieved. This PDL is achieved by designing the rather large but still reasonably misalignment-insensitive active area for PMUT, and the proper design of high-Q matching inductors. Moreover, for the first time, we demonstrated an instantaneous PDL_{DC}=3.46 mW power delivery to a DC load with an AlN PMUT receiver which is at least two orders of magnitude higher than other works. Moreover, the DC voltages up to 3.9V were measured without using a voltage-doubler or transformer as used in [5], [6], by using a parallel matching inductor and the custom-designed ASIC.

TABLE I
Summary of Specifications and Comparison

ALN-PMUT RX	This Work	[6]	[7]	[4]	[5]
Area (mm^2)	25	2.55	29	29	12.5
f_c (MHz)	2.5	3	2.5	2.5	0.7
$PDL_{AC}(\mu W)$*	6420	21.6	0.5	N/A	3600
$\eta_{RX,AC}$ (%)	7.13	0.24	0.01	N/A	8
Matching Network	Yes	Yes	No	No	Yes
$PDL_{DC}(\mu W)$*	3460	9.7	N/A	79	N/A
$\eta_{RX,DC}$ (%)	3.84	0.11	N/A	0.75	N/A
Inst. DC Power	Yes	No	No	No	Yes
PMU	ASIC	OTS	No	ASIC	OTS
Monolithic Integ.	No	No	No	Yes	No

* Normalized for an acoustic intensity of 0.5 $I_{max} = 360\ mW/cm^2$

References

[1] T. C. Chang, M. J. Weber, J. Charthad, S. Baltsavias, and A. Arbabian, "End-to-end design of efficient ultrasonic power links for scaling towards submillimeter implantable receivers," *IEEE transactions on biomedical circuits and systems*, vol. 12, no. 5, pp. 1100–1111, 2018.

[2] A. Rashidi, M. Zamani, T. Mondal, S. Hosseini, K. Laursen, B. Corbet, and F. Moradi, "Ultrasonically powered and controlled microsystem for dual-wavelength optogenetics with a multi-load regulation scheme," *IEEE Solid-State Circuits Letters*, 2023.

[3] L. Tacchetti, W. A. Serdijn, and V. Giagka, "An ultrasonically powered and controlled ultra-high-frequency biphasic electrical neurostimulator," in *2018 IEEE Biomedical Circuits and Systems Conference (BioCAS)*, pp. 1–4, ISSN: 2163-4025.

[4] O.-Y. Wong, D. Tabruyn, V. Rochus, and N. Van Helleputte, "An implantable power extraction circuit with integrated pmuts for wireless power delivery," in *ESSCIRC 2022-IEEE 48th European Solid State Circuits Conference (ESSCIRC)*. IEEE, 2022, pp. 217–220.

[5] B. Herrera, P. Simeoni, G. Giribaldi, L. Colombo, and M. Rinaldi, "Scandium-doped aluminum nitride pmut arrays for wireless ultrasonic powering of implantables," *IEEE Open Journal of Ultrasonics, Ferroelectrics, and Frequency Control*, vol. 2, pp. 250–260, 2022.

[6] Z. Rong, M. Zhang, Y. Ning, and W. Pang, "An ultrasound-induced wireless power supply based on aln piezoelectric micromachined ultrasonic transducers," *Scientific Reports*, vol. 12, no. 1, p. 16174, 2022.

[7] A. Proto, L. Rufer, S. Basrour, and M. Penhaker, "Modeling and measurement of an ultrasound power delivery system for charging implantable devices using an aln-based pmut as receiver," *Micromachines*, vol. 13, no. 12, p. 2127, 2022.

[8] M. Sacchet, R. van Schaijk, S. Kawasaki, J. H. Klootwijk, A. Rashidi, V. Giagka, A. S. Savoia, and R. Dekker, "Phase distribution efficiency of cm-scale ultrasonically powered receivers," in *Proc. IEEE International Ultrasonics Symposium*, in press.